Hydrol. Earth Syst. Sci. Discuss., 10, 1041–1070, 2013
www.hydrol-earth-syst-sci-discuss.net/10/1041/2013/
doi:10.5194/hessd-10-1041-2013

Hydrology and Earth System Sciences Discussions

Tracing groundwater salinization processes in coastal aquifers: a hydrogeochemical and isotopic approach in Na-Cl brackish waters of north-western Sardinia, Italy

G. Mongelli[1], S. Monni[2], G. Oggiano[2], M. Paternoster[1], and R. Sinisi[2]

[1]Department of Sciences, Campus di Macchia Romana, University of Basilicata, 85100 Potenza, Italy
[2]Department of Nature and Earth Sciences, University of Sassari, via Piandanna 4, 07100 Sassari, Italy

Received: 7 January 2013 – Accepted: 17 January 2013 – Published: 24 January 2013

Correspondence to: M. Paternoster (michele.paternoster@unibas.it)

Published by Copernicus Publications on behalf of the European Geosciences Union.

Abstract

In the Mediterranean area the demand of good quality water is often threatened by salinization, especially in coastal areas. The salinization is the result of concomitant processes due to both marine water intrusion and rock-water interaction, which in some cases are hardly distinguishable. In northwestern Sardinia, in the Nurra area, salinization due to marine water intrusion has been recently evidenced as consequence of bore hole exploitation. However, the geology of the Nurra records a long history from Paleozoic to Quaternary, resulting in relative structural complexity and in a wide variety of lithologies, including Triassic evaporites. To elucidate the origin of the saline component in the Nurra aquifer, may furnish a useful and more general model for the salinization processes in the Mediterranean area, where the occurrence of evaporitic rocks in coastal aquifers is a common feature. In addition, due to intensive human activities and recent climatic changes, the Nurra has become vulnerable to desertification and, similarly to other Mediterranean islands, surface-water resources can periodically suffer from drastic shortage.

With this in mind we report new data, regarding brackish waters of Na-Cl type of the Nurra, including major ions and selected trace elements (B, Br, I and Sr) and isotopic data, including $\delta^{18}O$, δD in water, and $\delta^{34}S$ and $\delta^{18}O$ in dissolved sulphate. To better depict the origin of the salinity we also analyzed a set of Nurra Triassic evaporites for mineralogical and isotopic composition. The brackish waters have Cl contents up to 2025 mg L^{-1} and the ratios between dissolved ions and chlorine, with the exception of the Br/Cl ratio, are not those expected on the basis of a simple mixing between rain water and seawater.

The $\delta^{18}O$ and δD data indicate that most of the waters are within the Regional Meteoric Water Line and the Global Meteoric Water Line supporting the idea that they are meteoric in origin. A relevant consequence of the meteoric origin of the Nurra Na-Cl type water is that the Br/Cl ratio, extensively used to assess the origin of salinity in fresh water, should be used with care also in near coastal carbonate aquifers. Overall,

HESSD

10, 1041–1070, 2013

and consistent with the geology and the lithological features of the study area, $\delta^{34}S$ and $\delta^{18}O$ in dissolved sulphate suggest that water-rock interaction is the responsible for the Nurra Na-Cl brackish water composition. Evaporites dissolution also explain the high chlorine contents since halite has been detected in the gypsum levels. Finally, the Nurra Na-Cl brackish water are undersaturated with respect to the more soluble salts involving, in a climate evolving toward semi-arid conditions, that the salinization process could dramatically intensify in the near future.

1 Introduction

In the Mediterranean area the demand of good quality water is rapidly increasing and the processes of salinization (e.g. Petalas and Lambrakis, 2006; El Yaouti et al., 2009; Ghiglieri et al., 2012; Sdao et al., 2012) often threaten the challenge for exploitation of water additional resources such as groundwaters. Salinization of aquifers in coastal areas is the result of concomitant processes due to both marine water intrusion and rock-water interaction, which in some cases are hardly distinguishable. In Sardinia, the Nurra area, which is located in the northwestern part of the island, has a coastline that stretchs up to 80 km (Fig. 1), and salinization due to marine water intrusion has been recently evidenced as consequence of bore hole exploitation (Ghiglieri et al., 2012). The geology of the Nurra records a long history from Paleozoic to Quaternary, resulting in relative structural complexity and in a wide variety of lithologies, including Variscan low-grade metamorphic basement consisting of phyllites, quartzites, and metabasites, lower-middle Permian continental sediments and volcanites, middle Triassic to Cretaceous red beds, evaporites and shallow-marine carbonate, lower Miocene ignimbrites, alluvial deposits of Messinian age, and alluvial and eolian Quaternary deposits (Mameli et al., 2007; Mongelli et al., 2012).

In the Nurra, notwithstanding the importance of local groundwater as the main source of good quality water, exploitation has been uncontrolled and, due to intensive human activities and recent climatic changes, the area has become vulnerable

HESSD
10, 1041–1070, 2013

to desertification (Ghiglieri et al., 2006). As a consequence, since the water demand is relevant and, similarly to other Mediterranean islands, surface-water resources can periodically suffer from drastic shortage (Ghiglieri et al., 2009).

Chemical data available for the Nurra aquifers (Ghiglieri et al., 2009) show these groundwaters are affected by a large chemical variability, including, for instance, TDS values (from 600 up to 4000 $mg\,L^{-1}$), chloride concentrations (from 3 up to 76 $mg\,L^{-1}$), and sulphate concentrations (from 0.2 up to 40 $mg\,L^{-1}$). This variability involves that various geochemical processes may affect the composition of the resource. Ghiglieri et al. (2009) suggested that the initial chemical composition of source water was conditioned by groundwater-rock interaction, including ion exchange with hydrothermal minerals and clays, incongruent solution of dolomite, and sulphate reduction. These statements, the relevance of the water resource and its role as strategic reserve in a climate evolving toward semiarid conditions, claim for a detailed study focusing on the processes determining the hydrogeochemistry of the Nurra groundwater and its quality, by tracking the sources of ions responsible for high salinity, aiming to assume the Nurra study case as a model for coastal aquifer hosted in Mesozoic carbonate-evaporite platform. In fact, the origin of the saline component of groundwaters is difficult to assess using only chemical data whereas coupling chemical and isotopic composition enhances our comprehension of the processes causing salinization of continental waters (e.g. Faye et al., 2005; Bouchaou et al., 2008; Gattacceca et al., 2009). With this in mind we report new data, regarding brackish waters of Na-Cl type of the Nurra, including major ions and selected trace elements (B, Br, I and Sr) and isotopic data, including $\delta^{18}O$, δD in water, and $\delta^{34}S$ and $\delta^{18}O$ in dissolved sulphate. To better depict the origin of the salinity we also analyzed a set of Nurra Triassic evaporites for mineralogical and isotopic composition.

HESSD
10, 1041–1070, 2013

2 Geological setting and groundwater circulation

The structural framework of north-western Sardinia mainly derives from its Mesozoic and Tertiary tectonic evolution (Combes et al., 1993; Mameli et al., 2007). This has to be related to the Bedoulian Movements, to the Pyrenean Phase and to the North Apennine collision followed by the opening of the Ligure-Provencal back arc basin (Carmignani et al., 2004; Mameli et al., 2007; Oggiano et al., 2009). The cover rocks are affected by NE–SW-trending folds and thrusts; evaporites commonly occur as décollement horizons and are exposed in the cores of anticlines and/or decòllement surfaces. Since the Burdigalian, the area was subjected to an extensional tectonic related to the opening of the Liguro-Provencal Basin, followed by moderate uplift during the Pliocene. As a whole Nurra, consists of a structural high that represents the uplifted part of a wide block, tilted to the east. To the west, the Nurra area borders the eastern passive margin of the Liguro-Provencal backarc basin; to the east, it abuts the edge of a N-S trending Miocene half-graben, the Porto Torres Basin (Thomas and Gennessaux, 1986; Funedda et al., 2000). The Mesozoic and Cenozoic structural evolution of the region resulted in a thin-skinned tectonics with the Mesozoic cover represented by a sequence made up of limestone, dolostone and, at a lesser extent, marlstones and evaporites that deformed independently from the Palaeozoic basement, which outcrops in the westernmost part of the region: in fact, as a whole, the older rock sequences are progressively exposed westward.

The middle Triassic succession at Nurra, rests on red beds of Permian-Triassic age and consists mainly of pure dolostones and limestones, with clay-rich beds occurring within the Triassic deposits as marly limestones, and clayey gypsum deposits. Marls also occur in the early and Late Jurassic strata, the former associated with dark Liassic limestone with euxinic facies and the latter with typical lagoonal-lacustrine “Purbeckian” facies (Pecorini, 1969). The most of Jurassic succession consists of limestones and dolostones with a thickness exceeding 700 m. The Jurassic beds host the most relevant aquifer of the area (Ghiglieri et al., 2009). Lower Cretaceous is represented by

HESSD
10, 1041–1070, 2013

pure Urgonian limestones, upper Cretaceous, lies unconformably on the Urgonian calcarenites along a bauxite level; it consists of Hippurites-bearing, limestones and marls of Late Cretaceous age (Coniacian to Maastrichtian). The whole Cretaceous beds have maximum thickness of about 400 m and host some perched aquifers out of the study area. In the study area the Mesozoic rocks are locally capped by Tertiary pyroclastic flows and by alluvial deposits of Messinian age, consisting of 30 to 80 m thick alluvial sequence mostly made up of clays and matrix-supported conglomerates. This deposit constitutes an important hydrogeologic unit for the north western part of the Nurra region since it acts as an aquitard that seals the confined aquifers hosted in the Mesozoic succession (Fig. 2).

The sampled area mostly pertains to the Porto Torres hydrogeological basin where the Jurassic aquifer has either reduced thickness in comparison to the Calich basin (Ghiglieri et al., 2009) or is absent toward the west. The groundwater flow in this basin is toward the northern shore (Asinara Gulf) whereas in the Calich basin is toward the south. The two hydrogeological systems are separated by a structural high toward which the axis of the main structures converge (B-B′ section in Fig. 2).

A detailed geological mapping of the area allow to recognize another structural high between Mount Zirra and Rocca della Bagassa which acts as geological watershed between the Calich basin and a small hydrogeological basin (Baratz Lake basin) flowing toward the western coast (Porto Ferro Gulf). The sampled waters pertain to the western part of the Porto Torres basin and to the Baratz Lake basin, within an aquifer hosted in Triassic carbonate rocks, cataclastic evaporite and sandstone (red beds). These saturated deposits are recharged by the Palaeozoic basement to the west and by the Jurassic carbonate hills to the east.

3 Sampling and analysis

Water samples from 19 springs and wells and two samples from the Baratz Lake were collected in September and October of 2011 in the coastal areas of the Nurra (Fig. 1).

HESSD
10, 1041–1070, 2013

In addition a seawater sample was collected from a site 0.1 km away from the Porto Ferro coastline and a rainwater sample was collected in September 2011 nearby the Baratz Lake site. Many of the sampled springs and wells are sources for drinking and irrigation waters. We used a high-resolution multiparametric probe (Hach HQ 30d) to measure the pH, temperature, and electrical conductivity (E.C.) of each sample.

All water samples were filtered through 0.45 µm MF-Millipore membrane filters in the field and stored in high-density polyethylene bottles (50 and 100 mL^{-1}). Prior to their use, these bottles were cleaned with nitric acid (HNO_3) and then rinsed with deionized water. The bottles were filled to the top with water, capped without leaving any head space, stored in a refrigerated container (~ 4 °C) during transportation to the laboratory, and kept cool until analysis. At each sampling site, two water samples (for cation analyses) were collected and acidified with Suprapur® HNO_3 (1 % v/v), after filtration, in order to prevent metal precipitation. For anion analysis, an un-acidified 100 mL^{-1} sample was collected. Alkalinity was determined in the field by titration with HCl (0.1 M). Cation concentrations (Ca, Mg, Na, K and Sr) were analyzed using Inductively Coupled Plasma-Optical Emission Spectroscopy (ICP/OES) at the Activation laboratory of Actlabs (Canada) with precision better than ±5 %. Anion concentrations were determined for Cl, SO_4, NO_3, and Br using ion chromatography (Dionex CX-100), and minor element (I and B) were determined using an inductively coupled plasma-mass spectrometry (ICP/MS). Ionic balance was computed for each sample taking into account major species. All samples exhibited imbalances lower than 5 %. Several certified reference materials (NIST 1643e, NIST 1640E and SLRS-5) were processed and analyzed along with the samples to assess the accuracy of our method. Our concentration measurements for these certified reference materials agree with the certified values. For oxygen isotopic analysis about 2 mL of each groundwater sample was equilibrated with CO_2 by shaking for 6 h at 25 °C (Epstein and Mayeda, 1953). For the hydrogen isotopic analysis, metallic zinc was used to produce hydrogen gas in the zinc reduction method (Coleman et al., 1982). Stable isotope ratios were measured on a dual inlet Finnigan Delta Plus IRMS with analytical precision of better than 0.2 ‰ for oxygen

HESSD
10, 1041–1070, 2013

and 1 ‰ for hydrogen. Five water samples calibrated with respect to V-SMOW and GISP International Standards were used as working standards. For the sulfur isotopic analysis, dissolved SO_4 was precipitated as $BaSO_4$ by addition of $BaCl_2$. The sample was then acidified to pH < 2 in order to dissolve any precipitated $BaCO_3$. For $\delta^{34}S$ analysis, SO_2 gas was prepared using the method of Yanagisawa and Sakai (1983). The isotopic composition of sulfur was determined using Continuous Flow-Isotope Ratio Mass Spectrometry (CF-EA-IRMS) at Isotope Science Laboratory of University of Calgary (ISL-UofC). The analytical precision is 0.3 ‰ for $\delta^{34}S$-(SO_4) and 0.5 ‰ for $\delta^{18}O$-(SO_4). Isotopic results were expressed as ‰ deviation (δ notation) relative to the international standards (V-SMOW for ^{18}O and ^{2}H, and V-CDT for ^{34}S and ^{18}O in dissolved SO_4; Gonfiantini et al., 1995). Finally, to properly evaluate the water-rock interaction processes a set of three evaporites was sampled and analyzed for mineralogical and isotopic composition. The mineralogy of bulk samples was obtained by X-ray powder diffraction (XRPD) using a Rigaku Rint 2200 diffractometer with CuKα radiation at 40 kV and 30 mA.

4 Results and discussion

4.1 Mineralogical and isotopic features of the Nurra evaporites

Three samples of evaporites of upper Triassic age have been analyzed for mineralogy and isotopic composition (Table 2; GR, GG and GB samples in Fig. 1). The rocks have been collected at the transition from Muschelkalk carbonates to Keuper evaporites where the alternance of grayish, whitish, and reddish evaporite levels, from older to younger, occur. All the evaporites are composed by gypsum; in the case of the grayish level XRD analyses reveal the presence of halite and quartz as minor components. The evaporites have $\delta^{34}S$-SO_4 values between +14.4 and +15.4 ‰ and $\delta^{18}O$-SO_4 values between +10.4 and +11.6 ‰ . These values are in the range of isotopic composition of

HESSD
10, 1041–1070, 2013

marine evaporites of upper Triassic age from +10.9 to +18.3 ‰ (Krouse and Grinenko, 1991 and references therein).

4.2 Water chemistry

Temperature, pH, EC (25 °C) values and the chemical compositions of water samples are provided in Table 1. The pH values range between 6.2 and 8.5, with the exception of the Baratz Lake samples (hereafter LB1 and LB2) which have higher values (9.2 and 8.2). Ambient water temperature is between 16.5 and 20.9 °C with the exception of the sample SP4 which show a value of 26.7 °C. The electrical conductivity ranges from 1240 to 7046 $\mu S\,cm^{-1}$. The amount of total dissolved solids (TDS) is usually in the 1–20 $g\,L^{-1}$ range, with the exceptions of the samples SP6 (TDS = 0.92 $g\,L^{-1}$) and CS2 (TDS = 0.98 $g\,L^{-1}$), and the water samples can be classified as brackish waters according to the classification of Drever (1997). The measured concentrations of major ions in the water samples are plotted on a Piper diagram (Fig. 3), which identifies the chemical compositions of the water samples as the Na-Cl type. In the anion concentration plot the samples are roughly distributed along the HCO_3-Cl edge, between the rain water and seawater points and fall close to the Cl apex.

In the diagrams ions vs. chlorine (Fig. 4) both the data of the Na-Cl water samples and the rainwater-seawater mixing line (hereafter RSML) are plotted to evaluate possible seawater intrusion. The Ca/Cl, SO_4/Cl, and Sr/Cl ratios in the water samples are much higher than expected on the basis of a simple mixing between rain water and seawater, thus suggesting that sulphate dissolution contributes to increasing the dissolved component. The Na/Cl is generally higher than that of the RMSL suggesting that dissolution of mineral phase(s) may contribute to add Na^+ to the solutions. The K/Cl is generally lower than that depicted by the RSML suggesting K^+ derives from silicate dissolution only. The variation in the boron contents are not correlated to the variation in the chlorine contents and the B/Cl ratio of the water samples is generally from lower to much lower than that of the RSML. Low values of the B/Cl ratio are associated to water-rock reaction, since Cl is preferentially leached with respect to B

HESSD
10, 1041–1070, 2013

and since B is adsorbed on clays (Leybourne et al., 2007). Halogens are retained as particularly useful to investigate the features of the saline component of groundwater (e.g. Boschetti et al., 2011). In the iodine vs. chlorine binary diagram the distribution of the water samples is scattered and most of them, characterized by a high I/Cl ratio, depart significantly from the RSML. Only in the bromine vs. chlorine binary diagram the water samples fit the RSML thus supporting the hyphothesis of a seawater intrusion. However, it has been stressed that the Br/Cl systematics of groundwaters is complex and that the Br/Cl ratio may not be a useful discriminator of marine and non-marine sources of salinity (Leybourne et al., 2007).

Finally, the NO_3 concentration of three water samples (PZ24 = 127 mg L^{-1}, PZ26 = 74 mg L^{-1}, CS5 = 91 mg L^{-1}) exceeds the maximum admissible concentration of 50 mg L^{-1} defined under Italian law (D.L. 31/2001). This claims for future and more detailed studies concerning environmental aspects. More in general, the lack of any significant (and positive) correlation of NO_3 with Cl ($r = -0.26$) and SO_4 ($r = -0.14$) exclude a nitrate origin associated to the salinization processes.

4.3 Isotopic composition of water and dissolved sulphate

The results of $\delta^{18}O$, δD, and oxygen and sulphur isotopes of dissolved sulphate analyses are presented in Table 2. Isotopic compositions of water samples range from −6.6 to −2.1 ‰ for $\delta^{18}O$ and from −39 to −16 ‰ for δD. The seawater sample gave a value of +1.1 ‰ for $\delta^{18}O$ and +5 ‰ for δD. Rainwater sample shows values of −5.5 ‰ for $\delta^{18}O$ and −29 ‰ for δD. Sulfate in the investigated groundwater samples is characterized by positive $\delta^{34}S$ and $\delta^{18}O$ values ranging between +15 and +21.2 ‰ and between +9 and +14.1, respectively.

Most of the waters, in the $\delta^{18}O$ vs. δD diagram, plot in a relatively tight cluster between the Regional Meteoric Water Line (RMWL, Chery, 1988; Celle et al., 2004) and the Global Meteoric Water Line (GMWL, Craig, 1961) suggesting they are meteoric in origin (Fig. 5). Lake water (LB1 and LB2 samples) and crop out waters (SP6, SP4, PZ18, PZ22) are enriched in the heavy O isotope forming a distinct subset (hereafter

HESSD
10, 1041–1070, 2013

LCO waters). These samples fall on a line with a slope of 4.96, which is considerably lower than that of the RMWL (about 8). Such low slope can be produced by evaporation effects (Rozansky and Frohlich, 2001) or mixing of groundwater and seawater. However the hypothesis of any mixing between groundwater and seawater (either due to recent seawater intrusion or to addiction of interstitial waters) is clearly ruled out by the Cl–δ^{18}O relationship (Fig. 6). The interstitial waters can be considered palaeofluids that had been trapped below the Miocene–Pleistocene sediments. In Fig. 6 mass-balance theoretical curves between values of rainwater (RW) and modern seawater (SW – data from this work) and rainwater and interstitial waters (IW) trapped in Miocene sediments (data from Böttcher et al., 1999) have been calculated and plotted together with the measured isotopic data. All samples fall away from the theoretical curves. In short, the δ^{18}O values together to chlorine contents show that there is no need to invoke an seawater source. This assumption is also supported by the lack of any correlation between distance from coastline and chlorine contents (Fig. 7).

4.4 The origin of salinity

As previously stated, both the elemental chemistry and the isotopic composition of groundwaters point toward an origin for the saline component not related to any seawater contribution. The concentration and isotopic composition of dissolved SO_4 in groundwater is related to both its source and mechanism of formation and the sulphur isotopes of dissolved sulphate can be used to identify the mixing of groundwaters of different origin (e.g. Schwarcz and Cortecci, 1974; Taylor and Wheeler, 1994; Ayora et al., 1995; Schulte et al., 1996). In addition, in an area where largely soluble salts, and especially gypsum, occur, the δ^{18}O-SO_4 values can be an useful tool for identifying sources of sulfate since the oxygen exchange between sulfate and water is extremely slow at low temperatures (Chiba and Sakai, 1985). Therefore, the δ^{18}O-SO_4 value usually remains unaltered after sulfate formation and hence reveals information about the formation process (Mayer et al., 1995; Van Donkelaar et al., 1995; Mitchell et al., 1998). Dual-isotope approach has been used with considerable success in both

HESSD
10, 1041–1070, 2013

surface water (e.g. Hitchon and Krouse, 1972; Krouse and Mayer, 2000; Robinson and Bottrell, 1997) and groundwaters (Moncaster et al., 2000; Gunn et al., 2006; Li et al., 2006; Bottrell, 2007). It is known that sulphate derived from dissolved evaporites always has positive δ^{34}S and δ^{18}O values, from +10 to +30 ‰ and from +12 to +20 ‰, respectively (Claypool et al., 1980), whereas sulphates from oxidation of sulphides or from biogenic emissions may have strongly negative δ^{34}S values (Yang et al., 1997). In Fig. 8 (δ^{34}S-SO_4 vs. δ^{18}O-SO_4 binary diagram), all investigated samples, including the LCO subset, fall in the field of marine evaporites (Clark and Fritz, 1997). A few samples are characterized by isotopic values consistent with those of the Upper Triassic Nurra evaporites (from +14.4 to 15.4 ‰ for δ^{34}S-SO_4 values and from +10.4 to +11.6 ‰ for δ^{18}O-SO_4 values) while others samples show higher values. The enrichment in measured ^{18}O and ^{34}S can either be induced by fractionation due to bacterial SO_4 reduction (Clark and Fritz, 1997) or derive from an isotopic heavier source. The lack of H_2S, the high Eh values, and the presence of dissolved O_2 (Ghiglieri et al., 2009 and references therein) exclude that these waters are affected by microbial SO_4 reduction. The isotopic heavier supply thus likely derives from the interaction with marine sediments of different age with respect to the upper Triassic (Keuper) Nurra evaporites (Fig. 8). Mass-balance curves between rainwater and evaporites of different Triassic age (Keuper, Muschelkalk, and Buntsandstein) support this hypothesis (Fig. 9) also in agreement with the occurrence of sediments of Triassic age in the investigated area.

Furthermore the presence of halite within the gypsum levels, as demonstrated by the XRD analysis, suggests that dissolution of evaporitic levels is responsible for the high chlorine abundances in the Nurra waters, also in agreement with the positive linear relationship existing between chlorine and sulphate contents ($r = 0.60$). In addition the saturation indexes for gypsum, anhydrite, halite and sylvite are below the unit (Table 2) suggesting the dissolution of soluble salts is an ongoing process. Finally this, in turn, involves that the salinization of the Nurra waters, in a climatic regime which evolves toward drier conditions, is a phenomenon that could be dramatically accentuated in the near future.

HESSD
10, 1041–1070, 2013

5 Summary

In the Nurra area occur brackish waters of the Na-Cl type composition which have Cl contents up to 2025 mg L^{-1}. The ratios between dissolved ions and chlorine, with the exception of the Br/Cl ratio, are not those expected on the basis of a simple mixing between rain water and seawater.

The $\delta^{18}O$ and δD data indicate that most of the waters are within the Regional Meteoric Water Line and the Global Meteoric Water Line supporting the idea that they are meteoric in origin. Due to evaporation few waters are ^{18}O-enriched.

A relevant consequence of the meteoric origin of the Nurra Na-Cl type water is that the Br/Cl ratio, extensively used to assess the origin of salinity in fresh water, and that in the present case is compatible with a seawater-rainwater mixing, thus erroneously supporting the hypothesis of a marine intrusion, should be used with care also in near coastal carbonate aquifers.

A dual-isotope approach based on $\delta^{34}S$ and $\delta^{18}O$ in dissolved sulphate proved to be useful in assess the origin of salinity in the Nurra Na-Cl brackish water. All investigated samples have isotopic composition within the isotopic range of marine evaporites. A few samples are characterized by isotopic values consistent with those of the upper Triassic (Keuper) Nurra evaporites that, in this study, were analyzed for the first time for isotopic and mineralogical composition. Others samples have heavier isotopic composition consistent with interaction with the isotopic composition of sediments of older Triassic age (Muschelkalk and Buntsandstein) also occurring in the area. Overall, and consistent with the geology and the lithological features of the study area, $\delta^{34}S$ and $\delta^{18}O$ in dissolved sulphate suggest that water-rock interaction is the responsible for the Nurra Na-Cl brackish water composition. Evaporites dissolution also explain the high chlorine contents since halite has been detected in the gypsum levels.

Finally, the Nurra Na-Cl brackish water are undersaturated with respect to the more soluble salts involving, in a climate evolving toward semi-arid conditions, that the salinization process could dramatically intensify in the near future.

HESSD
10, 1041–1070, 2013

Acknowledgements. The paper was financially supported by Banco di Sardegna Foundation and G. Mongelli and M. Paternoster grant (RIL 2009). Many thanks to A. Bonomo for her support during fieldwork.

References

Ayora, C., Taberner, C., Pierre, C., and Pueyo, J.: Modelling the sulfur and O isotopic composition of sulfates through a halite-potash sequence – implications for the hydrological evolution of the Upper Eocene South-Pyrenean Basin, Geochim. Cosmochim. Acta, 59, 1799–1808, 1995.

Böttcher, M. E., Bernasconi, S. M., and Brumsack, H. J.: Carbon, sulfur, and oxygen isotope geochemistry of interstitial waters from the western Mediterranean, in: Proc. ODP, Sci. Results, 161, Ocean Drilling Program, College Station, TX, 413–422, 1999.

Boschetti, T., Toscani, L., Shouakar-Stash, O., Iacumin, P., Venturelli, G., Mucchino, C., and Frape, S. C.: Salt waters of the Northern Apennine foredeep basin (Italy): origin and evolution, Aquat. Geochem., 17, 71–108, doi:10.1007/s10498-010-9107-y, 2011.

Bottrell, S. H.: Stable isotopes in aqueous sulphate as tracers of natural and contaminant sulphate sources: a reconnaissance study of the Xingwen karst aquifer, Sichuan, China, in: Natural and Anthropogenic Hazards in Karst Areas: Recognition, Analysis and Mitigation, 279, Special Publication, Geological Society, London, 123–135, 2007.

Bouchaou, L., Michelot, J. L., Vengosh, A., Hsissou, Y., Qurtobi, M., Gaye, C. B., Bullen, T. D., and Zuppi, G. M.: Application of multiple isotopic and geochemical tracers for recharge, salinization, and residence time of water in the Souss-Massa aquifer, southwest of Morocco, J. Hydrol., 352, 267–287, 2008.

Carmignani, L., Funedda, A., Oggiano, G., and Pasci, S.: Tectonosedimentary evolution of southwest Sardinia in the Paleogene: Pyrenaic or Apenninic dynamic?, Geodin. Acta, 17, 275–287, 2004.

Celle, H., Gonfiantini, R., Travi, Y., and Sol, B.: Oxygen-18 variations of rainwater during precipitation: application of the Rayleigh model to selected rainfalls in Southern France, J. Hydrol., 289, 165–177, doi:10.1016/j.jhydrol.2003.11.017, 2004.

HESSD

10, 1041–1070, 2013

Cherry, L.: Essai de caractérisation géochimique et isotopique d'émergences de circulations profondes dans deux types de massifs granitiques: Auriat (Creuse) et La Sposata (Corse), Ph.D. dissertation, Université de Paris-Sud, Orsay, 1988.
Chiba, H. and Sakai, H.: Oxygen isotope exchange between dissolved sulfate and water at hydrothermal temperatures, Geochim. Cosmochim. Acta, 49, 993–1000, 1985.
Clark, I. and Fritz, P.: Environmental Isotopes in Hydrogeology, Lewis Publications, Boca Raton, 328 pp., 1997.
Claypool, G. E., Holser, W. T., Kaplan, Y. R., Sakai, H., and Zak, I.: The age of sulfur and oxygen isotopes in marine sulfate and their mutual interpretation, Chem. Geol., 28, 199–260, 1980.
Coleman, M. L., Stephen, T. J., Durham, J. J., Rousse, J. B., and Moore, G. R.: Reduction of water with zinc for hydrogen analysis, Ann. Chem., 54, 993–995, 1982.
Combes, P. J., Oggiano, G., and Temussi I.: Géodynamique des bauxites sardes, typologie, genèse et contrôle paléotectonique, C.R. Acad. Sci., 316, 403–409, 1993.
Craig, H.: Isotopic variations in meteoric waters, Science, 133, 1702–1703, 1961.
D.L. 31/2001: Decreto legislativo 2 febbraio 2001, n. 31, attuazione della direttiva 98/83/CE relativa alla qualità delle acque destinate al consumo umano, available at: http://www.camera.it/parlam/leggi/deleghe/01031dl.htm, last access: January 2013, Gazzetta Ufficiale n. 52 del 3 March 2001.
El Yaouti, F., El Mandour, A., Khattach, D., Benavente, J., and Kaufmann, O.: Salinization processes in the unconfined aquifer of Bou-Areg (NE Morocco): a geostatistical, geochemical and tomographic study, Appl. Geochem., 24, 16–31, 2009.
Epstein, S. and Mayeda, T. K.: Variations of the $^{18}O/^{16}O$ ratios in natural waters, Geochim. Cosmochim. Acta, 4, 213–224, 1953.
Faye, S., Maloszewki, P., Stichler, W., Trimborn, P., Cisse Faye, S., and Bécaye Gaye, C.: Groundwater salinization in the saloum (Senegal) delta aquifer: minor elements and isotopic indicators, Sci. Total Environ., 343, 243–259, 2005.
Funedda, A., Oggiano, G., and Pasci, S.: The Logudoro basin: a key area for the Tertiary tectono-sedimentary evolution of North Sardinia, Boll. Soc. Geol. It., 119, 31–38, 2000.
Gattacceca, J. C., Vallet-Coulomb, C., Mayer, A., Claude, C., Radakovitch, O., Conchetto, E., and Hamelin, B.: Isotopic and geochemical characterization of salinization in the shallow aquifers of a reclaimed subsiding zone: the southern venice lagoon coastland, J. Hydrol., 378, 46–61, 2009.

HESSD
10, 1041–1070, 2013

Ghiglieri, G., Barbieri, G., and Vernier, A.: Studio Sulla Gestione Sostenibile Delle Risorse Idriche: Dall'Analisi Conoscitiva Alle Strategie di Salvaguardia e Tutela, ENEA, Rome, 550 pp., 2006.

Ghiglieri, G., Oggiano, G., Fidelibus, M. D., Alemayehu, T., Barbieri, G., and Vernier, A.: Hydrogeology of the Nurra region, Sardinia (Italy): basement-cover influences on groundwater occurrence and hydrogeochemistry, Hydrogeol. J., 17, 447–466, 2009.

Ghiglieri, G., Carletti, A., and Pittalis, D.: Analysis of salinization in the coastal carbonate aquifer of Porto Torres (NW Sardinia, Italy), J. Hydrol., 432–433 , 43–51, doi:10.1016/j.jhydrol.2012.02.016, 2012.

Gonfiantini, R., Stichler, W., and Rozanski, K.: Standards and intercomparison materials distributed by the IAEA for stable isotope measurements, in: Reference and Intercomparison Materials for Stable Isotopes of Light Elements, TECDOC 825, I.A.E.A., Vienna, 13–29, 1995.

Gunn, J., Bottrell, S. H., Lowe, D. J., and Worthington, S. R. H.: Deep groundwater flow and geochemical processes in limestone aquifers: evidence from thermal waters in Derbyshire, England, UK, Hydrogeol. J., 14, 868–881, 2006.

Hitchon, B. and Krouse, H. R.: Hydrogeochemistry of the surface waters of the Mackenzie River drainage basin, Canada: III. Stable isotopes of oxygen, carbon and sulphur, Geochim. Cosmochim. Acta, 36, 1337–1357, 1972.

Krouse, H. R. and Grinenko, V. A.: Stable Isotopes, Natural and Anthropogenic Sulphur in the Environment, SCOPE 43, John Wiley and Sons, Chichester, New York, Brisbane, Toronto and Singapore, 440 pp., 1991.

Krouse, H. R. and Mayer, B.: Sulphur and oxygen isotopes in sulphate, in: Environmental Tracers in Subsurface Hydrology, edited by: Cook, P. G. and Herczeg, A. L., Kluwer Academic, 195–231, 2000.

Leybourne, M. I. and Goodfellow, W. D.: Br/Cl ratios and O, H, C, and B isotopic constraints on the origin of saline waters from eastern Canada, Geochim. Cosmochim. Acta, 71, 2209–2223, 2007.

Li, X., Masuda, H., Kusakabe, M., Yanagisawa, F., and Zeng, H.: Degradation of groundwater quality due to anthropogenic sulfur and nitrogen contamination in the Sichuan Basin, China, Geochem. J., 40, 309–332, 2006.

HESSD
10, 1041–1070, 2013

Mameli, P., Mongelli, G., Oggiano, G., and Dinelli, E.: Geological, geochemical and mineralogical features of some bauxite deposits from Nurra (Western Sardinia, Italy): insights on conditions of formation and parental affinity, Int. J. Earth Sci., 96, 887–902, 2007.
Mayer, B., Fritz, P., Prietzel, J., and Krouse, H. R.: The use of stable sulfur and oxygen isotope ratios for interpreting the mobility of sulfate in aerobic forest soils, Appl. Geochem., 10, 161–173, 1995.
Mitchell, M. J., Krouse, H. R., Mayer, B., Stam, A. C., and Zhang, Y.: Use of stable isotopes in evaluating sulfur biogeochemistry of forested ecosystems, in: Isotopes Tracers in Catchment Hydrology, edited by: Kendall, C. and McDonnell, J. J., Elsevier, Amsterdam, 89–518, 1998.
Moncaster, S. J., Bottrell, S. H., Tellam, J. H., Lloyd, J. W., and Konhauser, K. O.: Migration and attenuation of agrochemical pollutants: insights from isotopic analysis of groundwater sulphate, J. Contam. Hydrol., 43, 147–163, 2000.
Mongelli, G., Mameli, P., Oggiano, G., and Sinisi, R.: Messinian palaeoclimate and palaeoenvironment in the western Mediterranean realm: insights from the geochemistry of continental deposits of NW Sardinia (Italy), Int. Geol. Rev., 54, 971–990, 2012.
Oggiano, G., Funedda, A., Carmignani, L., and Pasci, S.: The Sardinia-Corsica microplate and its role in the Northern Apennine Geodynamics: new insights from the Tertiary intraplate strike-slip tectonics of Sardinia, Ital. J. Geosci., 128, 527–539, 2009.
Otero, N. and Soler, A.: Sulfur isotopes as tracers of the influence of potash mining in groundwater salinisation in the Llobregat Basin (NE Spain), Water Res., 36, 3989–4000, 2002.
Pecorini, G.: Le Clavatoracee del "Purbeckiano" di Cala d'Inferno nella Nurra di Alghero (Sardegna nord-occidentale), Boll. Soc. Sarda Sc. Nat., 5, 1–14, 1969.
Petalas, C. and Lambrakis, N.: Simulation of intense salinization phenomena in coastal aquifers – the case of the coastal aquifers of Thrace, J. Hydrol., 324, 51–64, 2006.
Robinson, B. W. and Bottrell, S. H.: Discrimination of sulfur sources in pristine and polluted New Zealand river catchments using stable isotopes, Appl. Geochem., 12, 305–319, 1997.
Rozanski, K. and Fröhlich, K.: Surface water, in: Environmental Isotopes in the Hydrological Cycle, 3, edited by: Mook, W. G., UNESCO/IAEA, Paris, 2001.
Schulte, U., Bergmann, A., Obermann, P., and Strauss, H.: The Isotopic Compositions of Dissolved and Solid Sulfur and Carbon Species in a Deep Confined Tertiary Aquifer, V. M. Goldschmidt Conference, Heidelberg, 31 March–4 April, J. Conf. Abstr., 1, Cambridge Publications, 553, 1996.

HESSD
10, 1041–1070, 2013

Schwarcz, H. P. and Cortecci, G.: Isotopic analyses of spring and stream water SO_4 from the Italian Alps and Apennines, Chem. Geol., 13, 285–294, 1974.
Sdao, F., Parisi S., Kalisperi, D., Pascale, S., Soupios, P., Lydakis-Simantiris, N., and Kouli, M.: Geochemistry and quality of the groundwater from the karstic and coastal aquifer of Geropotamos River Basin at north-central Crete, Greece, Environ. Earth Sci., 67, 1145–1163, 2012.
Taylor, B. E. and Wheeler, M. C.: Sulfur- and oxygen-isotope geochemistry of acid mine drainage in the Western United States – field and experimental studies, in: Environmental Geochemistry of Sulfide Oxidation, edited by: Alpers, C. N. and Blowes, D. W., Am. Chem. Soc. Symp. Ser., 550, 481–514, 1994.
Thomas, B. and Gennesseaux, M.: A two stage rifting in the basin of Corsica-Sardinia strait, Mar. Geol., 72, 225–239, 1986.
Van-Donkelaar, C., Hutcheon, I. E., and Krouse, H. R.: $\delta^{34}S$, $\delta^{18}O$, δD in shallow groundwater: tracing anthropogenic sulfate and accompanying groundwater/rock interactions, Water Air Soil Poll., 79, 279–298, 1995.
Yanagisawa, F. and Sakai, H.: Thermal decomposition of barium sulfate–vanadium pentoxide–silica glass mixtures for preparation of sulfur dioxide in sulfur isotope ratio measurements, Anal. Chem., 55, 985–987, 1983.
Yang W., Spencer, R. J., and Krouse, H. R.: Stable isotope compositions of waters and sulfate species therein, Death Valley, California, USA; implications for inflow and sulfate sources, and arid basin climate, Earth Planet. Sc. Lett., 147, 69–82, 1997.

HESSD
10, 1041–1070, 2013

Table 1. Location of sampling points (water and rock) and chemical composition of the investigated waters.

Code	type	Lat. north	Long. east	Altitude m a.s.l.	Distance km	Temp. °C	pH	E.C. ms cm^{-1}	TDS g L^{-1}	HCO_3 mg L^{-1}	SO_4 mg L^{-1}	Cl mg L^{-1}	NO_3 mg L^{-1}
PZ2	w	4515601	1437197	79	7.2	20.8	6.9	3340	2.6	560	127	1040	14.8
PZ10	w	4516844	1438192	62	5.7	18.6	6.2	5200	4.4	79	284	2520	9.5
PZ14	w	4505469	1439048	51	5.8	19.1	7.3	1480	1.3	305	114	488	13.8
PZ17A	w	4505020	1438758	67	5.6	19.8	6.5	3150	2.4	180	179	1190	22.4
PZ18	cow	4505537	1434524	59	2.2	18.6	6.9	2380	2.0	177	239	858	0.4
PZ20	w	4505344	1436950	90	4.1	19.0	7.2	3310	2.7	274	223	1300	1.3
PZ22	cow	4502105	1433921	50	1.7	20.9	8.5	2960	2.8	465	385	1030	1.1
PZ23	w	4502415	1436039	45	3.8	18.8	6.8	4900	4.0	329	327	1890	19.0
PZ24	w	4507880	1439131	103	6.8	17.5	7.1	2240	2.1	329	197	749	127
PZ26	w	4520384	1439713	45	3.1	19.9	7.3	1240	1.2	329	125	295	74
SG3	S	4517964	1434592	67	2.1	20.6	8.2	4400	3.4	159	245	1700	32.6
CS1E	w	4517989	1439509	46	4.2	17.4	7.0	4015	2.3	183	294	995	2.9
CS2	w	4519852	1439112	49	3.1	18.1	7.1	1769	1.0	138	79	405	36.0
CS4	w	4518702	1439550	56	3.7	18.8	7.2	7046	4.0	146	218	2123	20.1
CS5	w	4518629	1439080	62	4.1	17.8	7.3	2472	1.5	177	176	564	91
CS5A	w	4518619	1439089	62	3.9	18.2	7.1	6073	3.7	153	480	1732	27.7
RB	S	4505216	1435411	51	2.6	17.2	7.8	2468	1.4	160	210	575	1.4
SP4	cow	4517963	1439377	42	4.4	26.7	8.0	3700	3.2	165	251	1720	1.3
SP6	cow	4519166	1438812	28	3.8	17.5	8.4	1574	0.9	140	80	367	0.4
LB2	lake	4503769	1434198	27	1.3	20.6	8.2	2320	1.5	210	190	620	0.3
LB1	lake	4503769	1434198	27	1.3	16.5	9.2	1960	1.6	232	216	655	0.4
RW	rain	4503769	1434198	27	n.m.	n.m.	6.3	28	0.05	12.0	24.1	3.3	0.2
SW	sea	4503469	1432531	0	n.m.	24.6	8.3	39 600	37.2	177	3040	20 900	0.1
GG	es	4516890	1444862	50	–	–	–	–	–	–	–	–	–
GB	es	4516890	1444862	50	–	–	–	–	–	–	–	–	–
GR	es	4516890	1444862	50	–	–	–	–	–	–	–	–	–

Note: w (well); s (spring); cow (crop out water); es (evaporite samples); E.C. (electrical conductivity at 25 °C); E. (electroneutrality); TDS (total dissolved solids); n.m. (not measured). The location of sampling points is provided in Gauss-Boaga coordinates; the distance is measured respect to coastline.

HESSD
10, 1041–1070, 2013

Table 1. Continued.

Code	K mgL^{-1}	Mg mgL^{-1}	Ca mgL^{-1}	Na mgL^{-1}	B μgL^{-1}	I μgL^{-1}	Br μgL^{-1}	Sr μgL^{-1}	E %
PZ2	17.6	114	187	527	164	7	4210	1420	0.8
PZ10	33.9	161	105	1200	172	9	8070	1200	−4.6
PZ14	13.4	47.5	48	303	149	7	1530	340	−3.7
PZ17A	11.1	78	63	680	97	6	3670	540	−1.5
PZ18	12.1	65	61	540	142	28	2960	490	0.1
PZ20	19.4	88	78	715	247	7	3980	650	−3.5
PZ22	16.1	25	30	865	258	7	3200	198	−3.6
PZ23	19.9	125	108	1170	184	12	6460	960	0.9
PZ24	9.5	60	126	459	142	20	2220	730	−2.0
PZ26	4.7	21.7	90	254	499	7	1340	270	−0.3
SG3	14.7	98	31.3	1080	135	12	5130	510	0.7
CS1E	2.9	65	197	578	213	42	3440	1010	4.1
CS2	8.9	30.8	92	180	143	5	1550	390	−2.4
CS4	20.3	158	249	1050	182	15	7080	1060	3.2
CS5	6.8	28	72	419	139	14	1870	230	0.7
CS5A	17.7	96	249	934	122	20	5850	1030	−0.3
RB	12.3	88	61	325	186	7	2270	470	3.2
SP4	14.1	100	190	782	178	2	5570	1620	−4.1
SP6	10.8	26.3	34.4	256	146	9	1590	320	3.3
LB2	14.6	71	50.1	359	164	5	2150	460	−1.2
LB1	12.8	78	40.5	402	127	14	2310	500	−1.1
RW	1.6	0.5	2.3	2.9	8	1	24	10.8	n.m.
SW	415	1330	458	10 900	5040	145	69 500	8250	−3.1
GG	–	–	–	–	–	–	–	–	–
GB	–	–	–	–	–	–	–	–	–
GR	–	–	–	–	–	–	–	–	–

Note: w (well); s (spring); cow (crop out water); es (evaporite samples); E.C. (electrical conductivity at 25 °C); E. (electroneutrality); TDS (total dissolved solids); n.m. (not measured). The location of sampling points is provided in Gauss-Boaga coordinates; the distance is measured respect to coastline.

HESSD
10, 1041–1070, 2013

Table 2. Isotopic data and saturation indexes for a few mineralogical phases.

Code	δ^{34}S-SO_4 ‰ V-CDT	δ^{18}O-SO_4 ‰ V-CDT	δ^{18}O ‰ V-SMOW	δD ‰ V-SMOW	SI Gypsum	SI Halite	SI Anhydrite	SI Sylvite
PZ2	17.4	12.2	−6.2	−34	−1.7	−5.0	−1.8	−6.0
PZ10	20.3	13.0	−6.4	−35	−1.7	−4.3	−1.9	−5.4
PZ14	14.9	12.7	−5.6	−34	−2.1	−5.5	−2.2	−6.4
PZ17A	17.0	13.3	−5.9	−36	−1.9	−4.8	−2.1	−6.2
PZ18	18.6	14.0	−5.0	−30	−1.7	−5.0	−1.9	−6.3
PZ20	15.5	10.2	−6.3	−36	−1.8	−4.7	−1.9	−5.9
PZ22	20.5	13.9	−5.1	−32	−1.9	−4.7	−2.1	−6.1
PZ23	19.5	13.0	−6.1	−36	−1.6	−4.4	−1.8	−5.8
PZ24	15.5	10.7	−6.4	−39	−1.5	−5.1	−1.7	−6.4
PZ26	16.2	10.7	−5.8	−34	−1.7	−5.8	−1.9	−7.1
SG3	20.2	13.7	−6.5	−38	−2.2	−4.4	−2.3	−5.9
CS1E	18.4	12.0	−5.7	−33	−1.2	−4.9	−1.4	−6.8
CS2	15.6	10.2	−6.6	−36	−1.9	−5.8	−2.1	−6.7
CS4	18.0	13.2	−6.1	−34	−1.4	−4.4	−1.6	−5.7
CS5	18.9	11.8	−6.4	−36	−1.7	−5.3	−1.9	−6.7
CS5A	20.9	14.1	−6.0	−35	−1.1	−4.5	−1.2	−5.8
RB	14.5	9.6	−6.0	−33	−1.8	−5.4	−1.9	−6.4
SP4	18.9	12.7	−3.3	−25	−1.4	−4.6	−1.6	−5.9
SP6	15.8	9.8	−3.1	−22	−2.3	−5.7	−2.4	−6.6
LB2	15.5	10.9	−2.4	−18	−1.9	−5.3	−2.1	−6.3
LB1	15.3	12.2	−2.1	−16	−1.9	−5.2	−2.1	−6.3
RW	3.7	10.0	−5.5	−29	–	–	–	–
SW	21.5	10.1	1.1	5	–	–	–	–
GG	14.4	11.6	n.m.	n.m.	–	–	–	–
GB	14.9	11.2	n.m.	n.m.	–	–	–	–
GR	15.4	10.4	n.m.	n.m.	–	–	–	–

Note: n.m. = not measured; saturation indexes were performed using by GWB® 8.0 with the thermodynamic database thermoddem.dat.

HESSD
10, 1041–1070, 2013

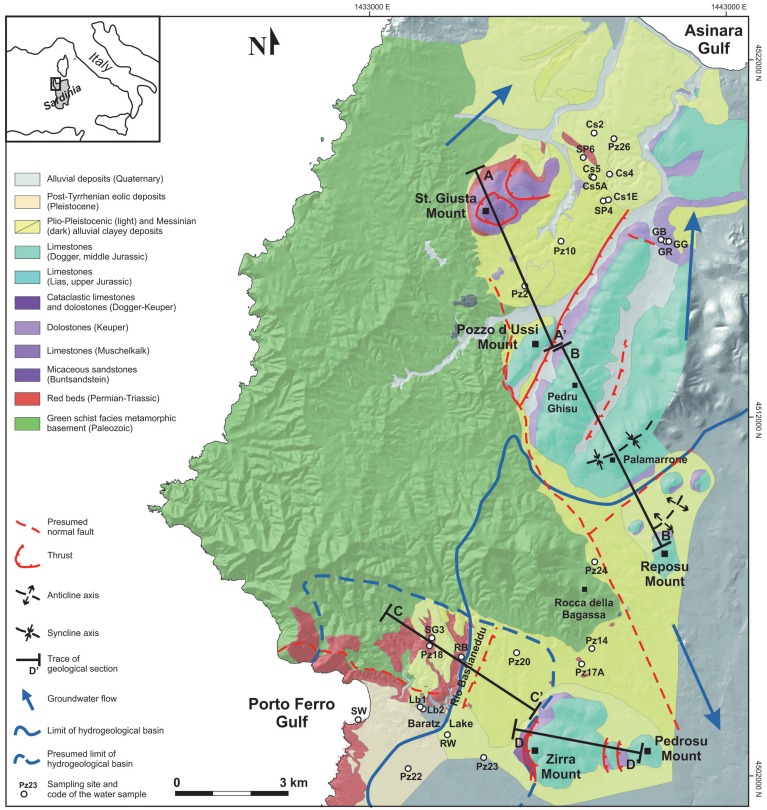

Fig. 1. DTM-base geological map of investigated area. The localization of sampling sites and code of the analyzed water and rock sample are shown. The limit of hydrogeological basins are from Ghiglieri et al. (2009). The blue arrows indicate the direction of prevailing groundwater flow. See text for further details.

HESSD
10, 1041–1070, 2013

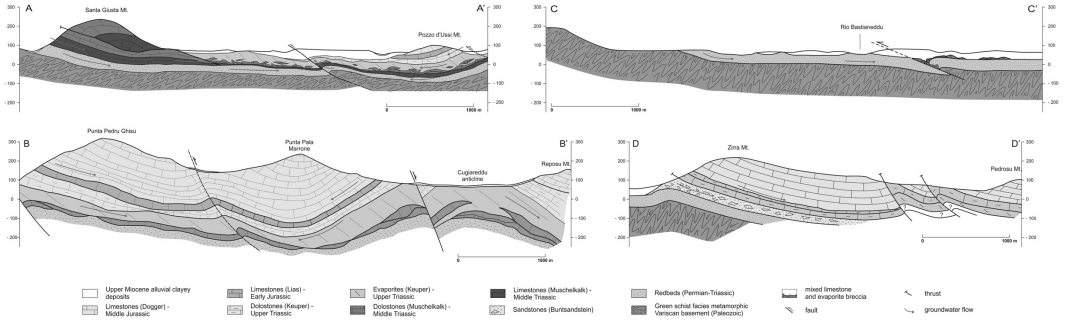

Fig. 2. A-A′, B-B′, C-C′ and D-D′ geological sections of Fig. 1. See text for further details.

HESSD
10, 1041–1070, 2013

Tracing groundwater salinization processes in coastal aquifers

G. Mongelli et al.

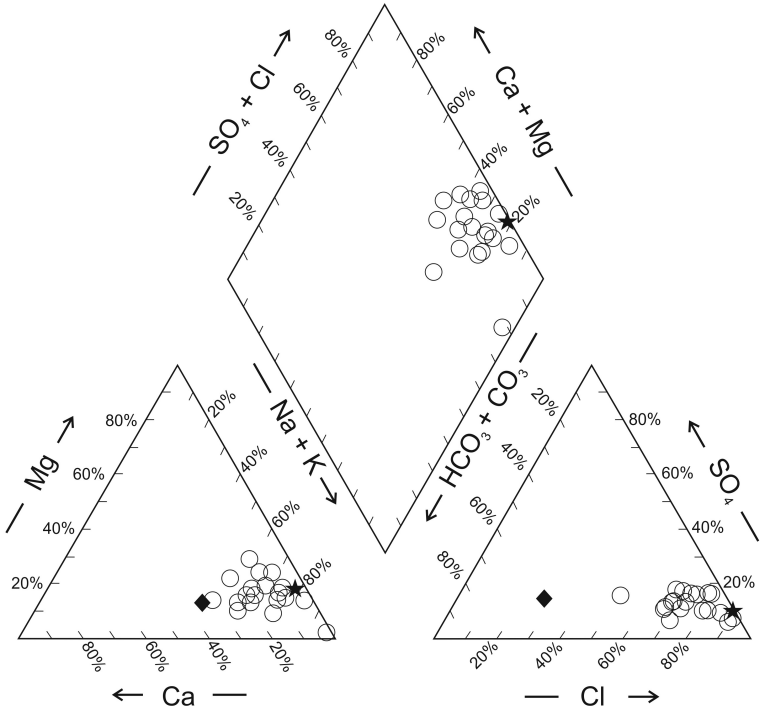

Fig. 3. Relative amounts of major ions analyzed in sampled waters plotted in a Piper plot. Filled diamonds = rain water; filled stars = seawater.

HESSD
10, 1041–1070, 2013

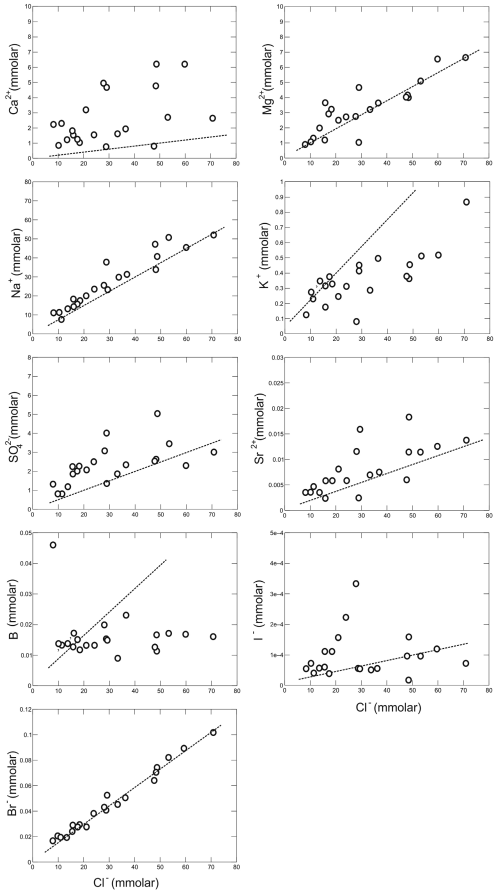

Fig. 4. Binary plots between chlorine and selected ions (expressed in mmol/l) in the analyzed water samples. The lines indicate mixing between marine and rainwater samples.

HESSD
10, 1041–1070, 2013

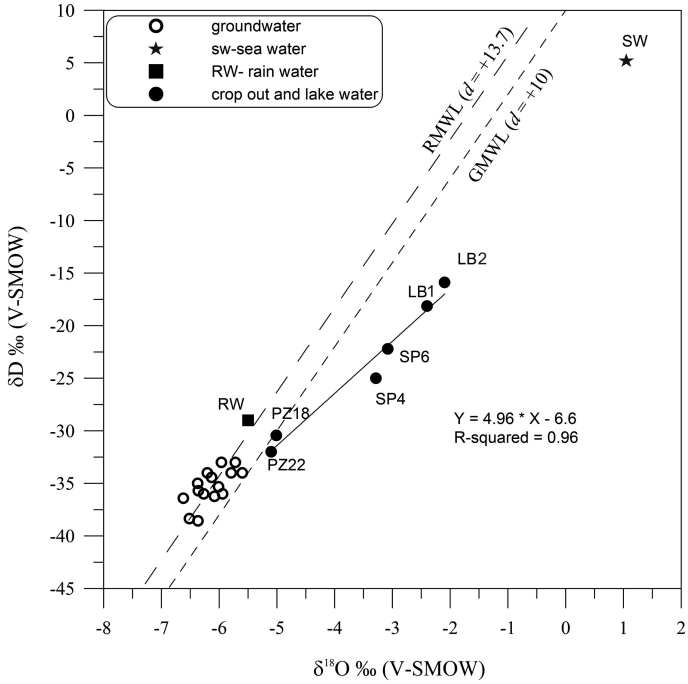

Fig. 5. δ^{18}O vs. δD diagram. The Regional Meteoric Water Line (RMWL Chery, 1988; Celle et al., 2004) and the Global Meteoric Water Line (GMWL; Craig 1961) are drawn for comparison. The equation describing the line produced by evaporation effects is also displayed.

HESSD
10, 1041–1070, 2013

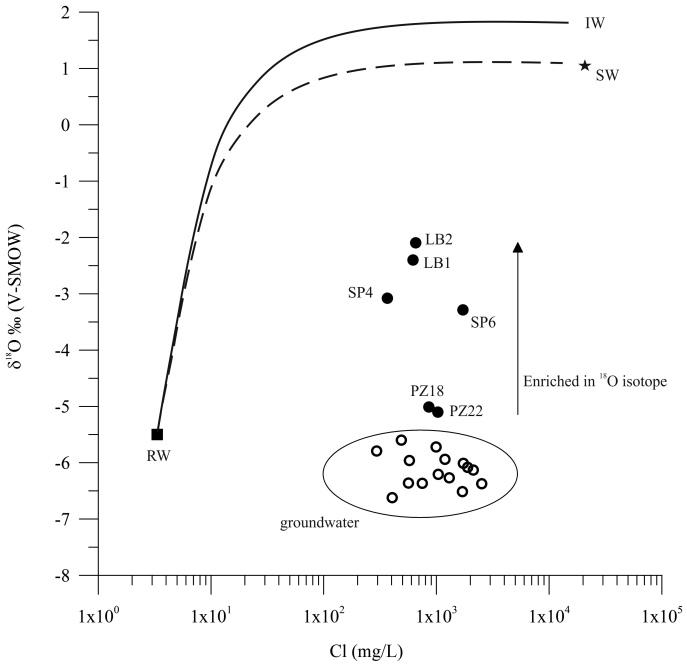

Fig. 6. δ^{18}O vs. Cl Mass-balance theoretical curves between values of rainwater (RW – data from this work) and modern seawater (SW – data from this work) and between rainwater and interstitial waters (IW) trapped in Miocene sediments (data from Bottcher et al., 1999) are shown. Isotopic values of the most Nurra waters remain constant with the exception of LCO waters. Anyway all samples fall away from the theoretical curves. The symbols are as in Fig. 5.

HESSD
10, 1041–1070, 2013

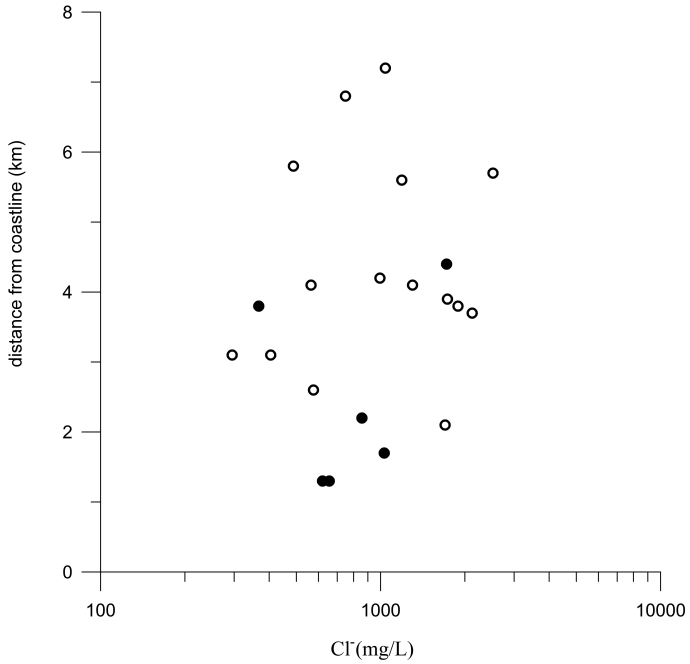

Fig. 7. Binary plot of Cl vs. distance from coastline.

HESSD
10, 1041–1070, 2013

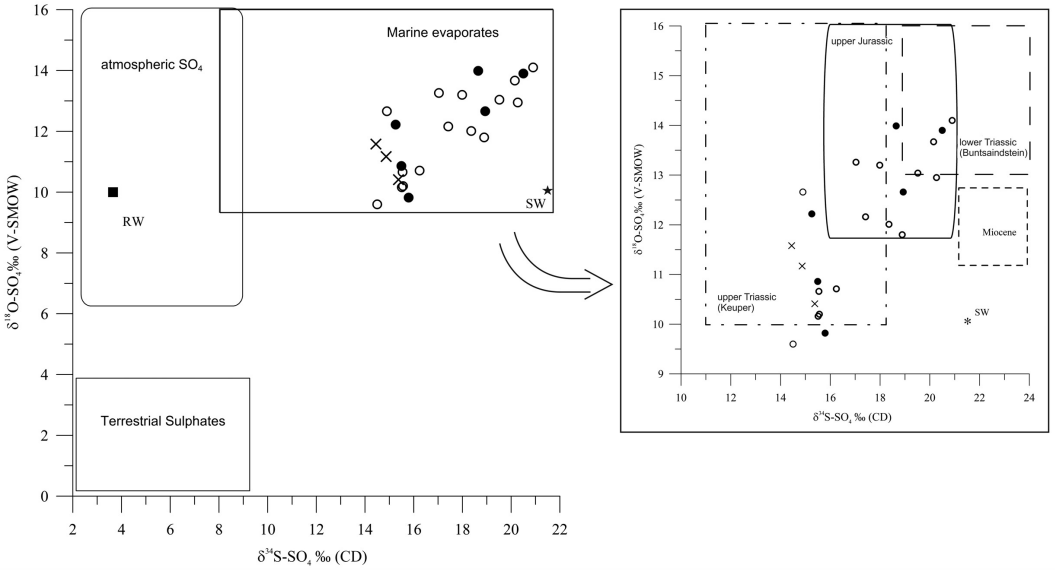

Fig. 8. Diagram of the δ^{34}S and δ^{18}O of dissolved sulphate. The isotopic composition data of various sources in the diagram are from Clark and Frits (1997). Additional data from Krouse and Grinenko (1991) have been used for the zoom of the diagram. The symbols are as in Fig. 5; the crosses represent the isotopic values of the Nurra evaporate samples.

HESSD
10, 1041–1070, 2013

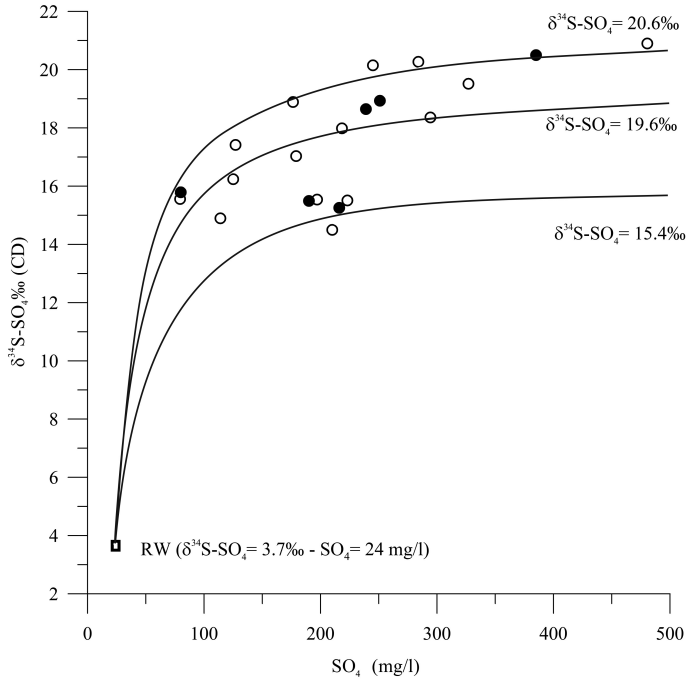

Fig. 9. Plot of $\delta^{34}S$ (SO_4) and SO_4 concentrations for the investigated waters. The Mass-balance theoretical curves (solid curve) between rainwater and Triassic evaporites are shown. The displayed isotopic and chemical data of rainwater (RW: $\delta^{34}S$ = +3.7‰ ; SO_4 = 24mg L^{-1}) refer to September 2011 sampling carried out near the Baratz Lake (see Fig. 1) while the data on Triassic evaporites are from Krouse and Grinenko (1991) and references therein ($\delta^{34}S$ = +15.4‰ is the average value for marine sulphates of Keuper; $\delta^{34}S$ = +19.6‰ is the average value for marine sulphates of Muschelkalk and $\delta^{34}S$ = +20.6 ‰ refer to marine sulphates of Buntsandstein). The symbols are as in Fig. 5.

HESSD
10, 1041–1070, 2013